

Entanglement of bosonic systems under monitored evolution

Quancheng Liu and Klaus Ziegler

*Department of Physics, Institute of Nanotechnology and Advanced Materials, Bar-Ilan University, Ramat Gan 52900, Israel
Institut für Physik, Universität Augsburg, D-86135 Augsburg, Germany*

(Dated: March 12, 2024)

The evolution of non-interacting bosons in the presence of repeated projective measurements is studied. Following the established approach, this monitored evolution is characterized by the first detected return and the first detected transition probabilities. We show that these quantities are directly related to the entanglement entropy and to the entanglement spectrum of a bipartite system. Calculations with specific values for the number of bosons, the number of measurements and the time step between measurements reveal a sensitive and often strongly fluctuating entanglement entropy. In particular, we demonstrate that in the vicinity of special values for the time steps the evolution of the entanglement entropy is either stationary or performs dynamical switching between two or more stationary values. In the entanglement spectrum, on the other hand, this complex behavior can be associated with level crossings, indicating that the dominant quantum states and their entanglement respond strongly to a change of the system parameters. We discuss briefly the role of time averaging to remove the fluctuations of the entanglement entropy.

I. INTRODUCTION

Repeated measurement on a quantum system has been used to determine the first detected return (FDR) to the initial state or the first detected transition (FDT) to a state that is different from the initial state. The idea is to prepare the quantum system in an initial state, let it evolve unitarily and perform at discrete times $\{j\tau\}_{j=1,2,\dots}$ projective measurements of a given state. If the measurement is successful, which means that the given state is detected, the experiment is stopped. If the measurement is unsuccessful, where the given state is not detected, the experiment continues by evolving another time step τ , followed by another measurement. After m unsuccessful measurements and another unitary evolution over time τ we eventually determine the probability of the system to be in a certain state [1]. This protocol has been applied to single-particle states to detect the particle location on a graph [2–8].

For the evolution of a system with more than one particle the entanglement of the quantum state is a fundamental effect. It can be characterized, for instance, by the Rényi entanglement entropy that measures the quantum correlations between two subsystems under a spatial bipartition [9–13]. Probing the entanglement entropy has become an important and popular concept to study measurement-induced entanglement transitions, to characterize the many-body evolution and many-body localization [14–29] and to classify the topology of quantum systems.

In this paper we will study the Rényi entanglement entropy in a system of non-interacting bosons, which is subject to periodically repeated projective measurements. This enables us to study the FDR/FDT probabilities as well as the entanglement entropy and entanglement spectrum, and to investigate the relation between both quantities.

The focus of this paper is on physical aspects of the monitored evolution that can also be applied to quantum computing [30]. Although quantum computing is typically based on qubits (i.e., spin states), potentially bosonic systems could also be used [31]. A promising example are photonic states. In particular, we consider N non-interacting bosons, distributed in two wells which are coupled by tunneling. This can be experimentally realized as a pair of photonic cavities that are coupled by an optical fiber [32–36]. The underlying Hilbert space is $N + 1$ -dimensional and enables us to study the scaling behavior of the entanglement with N .

The structure of the paper is that in Sect. II we provide a general theory part with the definitions of the FDR/FDT probabilities and their relations to the reduced density matrix, the entanglement entropy and the entanglement spectrum. More details for the calculation of the FDR/FDT probabilities are provided in Sect. II A. This includes an approach that connects the monitored evolution due to repeated measurements to the unitary evolution. The reader, who is not interested in the theoretical concepts but more in the results of the monitored evolution, can skip this section. Then in Sect. III our approach to the monitored evolution is applied to the tunneling of N non-interacting bosons in a double well. For this specific model the eigenvalues and spectral weights are calculated. Finally, in Sect. IV specific examples in terms of the parameters of the model are presented for the entanglement entropy and the entanglement spectrum.

II. GENERAL CONCEPT OF PROJECTED MEASUREMENTS

The quantum system is characterized by the density operator that reads in the presence of repeated projective measurements

$$\rho^m(\tau) = \frac{1}{\mathcal{N}} e^{-iH\tau} (\Pi e^{-iH\tau})^{m-1} |\psi_0\rangle \langle \psi_0| (e^{iH\tau} \Pi)^{m-1} e^{iH\tau} \quad (1)$$

with the normalization $\mathcal{N} = \text{Tr}[e^{-iH\tau} (\Pi e^{-iH\tau})^{m-1} |\psi_0\rangle \langle \psi_0| (e^{iH\tau} \Pi)^{m-1} e^{iH\tau}]$. This density operator describes a quantum walk [37], where after each time steps τ a projective measurement Π is applied. The latter prevents the visit of the Hilbert space after a time step τ that is orthogonal to the Π -projected Hilbert space. Although we can choose Π freely, we will consider below a special choice within the Fock basis of our model, where the orthogonal projection Π into a N -dimensional subspace.

For the following discussion we consider a product space $\mathcal{H}_1 \otimes \mathcal{H}_2$ which is spanned by the basis $\{|n, N-n\rangle\}_{0 \leq n \leq N}$. This should be understood as a basis for n particles in \mathcal{H}_1 and $N-n$ particles in \mathcal{H}_2 , where the total number of particles N is fixed. The basis states can also contain additional quantum numbers, which are not relevant for the general discussion. In Sect. III we will consider the special case in which the product Hilbert space represents a double well, where n bosons are in the left and $N-n$ bosons are in the right well. Then the basis consists of Fock states $|n, N-n\rangle \equiv |n\rangle |N-n\rangle$ without additional quantum numbers.

Returning to the general case, in the basis $\{|n, N-n\rangle\}_{0 \leq n \leq N}$ the $(N+1) \times (N+1)$ density matrix reads $\rho_{n, N-n; n', N-n'}^m = \langle n, N-n | \rho^m(\tau) | n', N-n' \rangle$ with $n, n' = 0, \dots, N$. After summing over all basis states of \mathcal{H}_2 the reduced density matrix $\hat{\rho}$ becomes an $(N+1) \times (N+1)$ diagonal matrix with elements

$$\begin{aligned} \hat{\rho}_{nn}^m &= \sum_{n'=0}^N \langle n, n' | \rho^m(\tau) | n, n' \rangle = \langle n, N-n | \rho^m(\tau) | n, N-n \rangle \\ &= \frac{1}{\mathcal{N}} \langle n, N-n | e^{-iH\tau} (\Pi e^{-iH\tau})^{m-1} |\psi_0\rangle \langle \psi_0| (e^{iH\tau} \Pi)^{m-1} e^{iH\tau} | n, N-n \rangle. \end{aligned} \quad (2)$$

With the projector $P_n := |n, N-n\rangle \langle n, N-n|$ the density matrix elements can also be written as a trace expression

$$\hat{\rho}_{nn}^m = \frac{1}{\mathcal{N}} \text{Tr} [P_n e^{-iH\tau} (\Pi e^{-iH\tau})^{m-1} P_0 (e^{iH\tau} \Pi)^{m-1} e^{iH\tau}], \quad (3)$$

where we have assumed $|\psi_0\rangle = |0, N\rangle$ for the initial state. One should note that the right-hand side of Eq. (2) with Π replaced by $\Pi_n = \mathbf{1} - P_n$ is either the first detected return (FDR) probability (for $n = 0$) or the first detected transition (FDT) probability (for $n > 0$). Therefore, known results of the FDR/FDT probabilities [6, 38, 39] can be directly used for the reduced density matrix through the relation

$$\hat{\rho}_{nn}^m = \frac{|\phi_{m;n0}|^2}{\sum_{n=0}^N |\phi_{m;n0}|^2} \quad (4)$$

with the FDT amplitude for $|0, N\rangle \rightarrow |n, N-n\rangle$ ($n \neq 0$) after m measurements

$$\phi_{m;n0} := \langle n, N-n | e^{-iH\tau} (\Pi_n e^{-iH\tau})^{m-1} | 0, N \rangle \quad (5)$$

and the corresponding FDR amplitude $\phi_{m;00}$ for $|0, N\rangle \rightarrow |0, N\rangle$. It is crucial to note that $\sum_{n=0}^N |\phi_{m;n0}|^2 \leq 1$ for $m > 1$ due to the projection Π . Some known results for the FDR/FDT amplitudes are summarized in Sect. II A.

With this expression for $\hat{\rho}_{nn}^m$ we can introduce the Rényi entropy [23] as a quantitative measure for the entanglement of the two Hilbert spaces \mathcal{H}_1 and \mathcal{H}_2

$$\mathcal{S}_\alpha(\tau, N, m) = \frac{1}{1-\alpha} \log_2 \text{Tr}[(\hat{\rho}^m)^\alpha(\tau)]. \quad (6)$$

In general, α is a free parameter and typical values used are $\alpha = 2, 3$ [23]. For the subsequent calculations we set $\alpha = 2$, i.e., we will calculate $\mathcal{S}_2(\tau, N, m)$ as the entanglement entropy (EE).

While the EE reveals a global measure for the monitored evolution, the entanglement spectrum (ES) [40] provides a local measure of the evolution for the transition between individual states $|0, N\rangle \rightarrow |n, N-n\rangle$. In other words, it reveals the contribution of individual states to the entangled state of the evolving quantum system. It is defined as

the logarithm of the reduced density matrix eigenvalues. In the present case the reduced density matrix is already diagonal, such that

$$\xi_{m;n} = -\log(\bar{\rho}_{nn}^m) = -2\log(|\phi_{m;n0}|) + \log\left(\sum_{n=0}^N |\phi_{m;n0}|^2\right). \quad (7)$$

The smallest value of $\xi_{m;n}$ corresponds with the dominant transition $|0, N\rangle \rightarrow |n, N-n\rangle$ after m measurements. A crossing of the lowest levels upon changing of the time step τ or m is reminiscent of a phase transition in classical statistical systems due to a crossing of the ground state energies.

The FDR/FDT amplitude in Eq. (5) is written in the Fock basis. It is convenient to express the evolution operator in the eigenbasis $\{|E_k\rangle\}$ of the Hamiltonian as

$$\phi_{m;n0} = \sum_{\{k_j=0\}}^N \langle \psi_n | E_{k_1} \rangle e^{-iE_{k_1}\tau} \langle E_{k_1} | \Pi_n | E_{k_2} \rangle e^{-iE_{k_2}\tau} \cdots \langle E_{k_{m-1}} | \Pi_n | E_{k_m} \rangle e^{-iE_{k_m}\tau} \langle E_{k_m} | \psi_0 \rangle. \quad (8)$$

For the projector $\Pi_n = \mathbf{1} - |n, N-n\rangle\langle n, N-n|$ a typical matrix element then reads

$$\langle E_k | (\mathbf{1} - |n, N-n\rangle\langle n, N-n|) | E_{k'} \rangle = \delta_{kk'} - q_{n,k}^* q_{n,k'} =: (\mathbf{1} - Q_n^* E Q_n)_{kk'} \quad (9)$$

with $q_{n,k} = \langle n, N-n | E_k \rangle$ and $q_{n,k}^* = \langle E_k | n, N-n \rangle$. E is the $(N+1) \times (N+1)$ matrix, whose matrix elements are 1. Moreover, Q_n is a diagonal matrix, consisting of the elements $\{q_{n,k}\}$. Then the FDR/FDT amplitude of Eq. (5) can be written as

$$\phi_{m;n0} = \sum_{k,k'=0}^N q_{n,k} D_k [(\mathbf{1} - Q_n^* E Q_n) D]_{kk'}^{m-1} q_{0,k'}^* \quad (10)$$

with $D_k = e^{-iE_k\tau}$. It should be noticed that $(Q_n^*)^{-1}(D - Q_n^* E Q_n D)^{m-1} Q_n^*$ is a function of $Q_n Q_n^*$ (cf. Ref. [41]): Since Q_n, D are diagonal matrices, they commute and we get the relation

$$(D - Q_n^* E D Q_n)^{m-1} = Q_n^* (D - E D Q_n Q_n^*)^{m-1} (Q_n^*)^{-1}, \quad (11)$$

which is proved by complete induction. Moreover, we can write $(D - Q_n^* E D Q_n)^{m-1} = D^{-1/2} T_n^{m-1} D^{1/2}$ with $T_n := D^{1/2} (\mathbf{1} - Q_n^* E Q_n) D^{1/2}$ and for Eq. (10)

$$\phi_{m;n0} = \text{Tr}(D^{1/2} T_n^{m-1} D^{1/2} Q_0^* E Q_n). \quad (12)$$

Thus, the matrix T_n represents the monitored evolution under repeated measurements, which is the analogue of the unitary evolution matrix $U = \exp(-iH\tau)$ in the Fock basis. Its largest eigenvalues control the large m (i.e., stationary) behavior of $\phi_{m;n0}$, while the smaller eigenvalues decay quickly. Therefore, the task is to identify those largest eigenvalues for the given parameters of the model.

The matrix T_n has some important properties that are useful for the calculation of $\phi_{m;n0}$. First, since $\sum_k q_{n,k} q_{n',k}^* = \delta_{nn'}$, there is a complete set of right/left eigenvectors of the Hermitean matrix $\mathbf{1} - Q_n^* E Q_n$ with an eigenvalue 0 and N eigenvalues 1 due to

$$\sum_{k'} (\delta_{kk'} - q_{n,k}^* q_{n,k'}) q_{n',k'}^* = (1 - \delta_{nn'}) q_{n',k}^* \text{ and } \sum_k q_{n',k} (\delta_{kk'} - q_{n,k}^* q_{n,k'}) = (1 - \delta_{nn'}) q_{n',k'}. \quad (13)$$

Defining the vector $\mathbf{q}_n := (q_{n,0}, q_{n,1}, \dots, q_{n,N})^T$, we get $Q_n^* E Q_n \mathbf{q}_{n'}^* = \mathbf{q}_n \delta_{nn'}$, which implies for the vector $\mathbf{x} := \sum_{n'} a_{n'} D^{-1/2} \mathbf{q}_{n'}^*$

$$T_n \mathbf{x} = \begin{cases} D \mathbf{x} & \text{for } a_n = 0 \\ 0 & \text{for } a_{n'} = 0 \text{ (} n' \neq n \text{)} \end{cases}. \quad (14)$$

It is possible that $T_n \mathbf{x} = D \mathbf{x}$ reduces to $T_n \mathbf{x} = e^{i\varphi} \mathbf{x}$ when we have $D \mathbf{x} = e^{i\varphi} \mathbf{x}$, which can happen in the presence of degenerate $E_j \tau \pmod{2\pi}$ or when some components of the vectors $\mathbf{q}_{n'}$ vanish. In this case \mathbf{x} is an eigenvector of T_n whose eigenvalue lies on the unit circle of the complex plane. This means that \mathbf{x} does not decay but accumulates only a phase. This eigenvector does not contribute to the FDR/FDT amplitude though, since \mathbf{x} is orthogonal to \mathbf{q}_n and, therefore, $E Q_n \mathbf{x} = 0$.

Besides these special vectors, the eigenvalues of T_n can be quite complex in general. On the other hand, even a two-level system (i.e., $N = 1$, $n = 0, 1$) with energies $E_{0,1}$ is already instructive. In this case T_n has two eigenvalues:

$$\lambda_0 = 0, \quad \lambda_1 = (1 - |q_{n,0}|^2)e^{-2iE_0\tau} + |q_{n,0}|^2e^{-2iE_1\tau}, \quad (15)$$

where $|q_{n,1}|^2 = 1 - |q_{n,0}|^2$ and $|\lambda_1|^2 = 1 - 2(1 - |q_{n,0}|^2)|q_{n,0}|^2(1 - \cos[2(E_1 - E_0)\tau])$. Thus, the eigenvalues of T_n are on the unit disk, one at the center and the other one only for special values on the unit circle, namely for $|q_{n,0}| = 0, 1$ and/or for $(E_1 - E_0)\tau = 0 \pmod{\pi}$. This means that, except for the special values with $|\lambda_1| = 1$, T_n^{m-1} decays exponentially fast. We will see subsequently that this type of behavior exists also for larger systems. In particular, we will study a system of N non-interacting bosons.

A. FDR/FDT amplitudes

Next we discuss the connection between the unitary and the monitored evolution by a linear relation. We consider only the FDR/FDT amplitude, since this is the building block for the other physical quantities, according to our discussion in the previous section. The ‘first detected passage time problem’, as discussed in Refs. [1, 4] for a single particle on a tight-binding graph, can be directly generalized to the evolution in a general Hilbert space. The unitary evolution of the transition $|\psi_0\rangle \rightarrow |\psi_n\rangle$ for the time τ provides the amplitudes

$$v_m := \phi_{0;n0}(m\tau) = \langle \psi_n | e^{-iHm\tau} | \psi_0 \rangle, \quad u_m := \phi_{0;00}(m\tau) = \langle \psi_0 | e^{-iHm\tau} | \psi_0 \rangle. \quad (16)$$

There exists a mapping from the unitary amplitudes in Eq. (16) to the FDR/FDT amplitudes $\phi_{t,m} := \phi_{m,1} = \langle \psi | (e^{-i\tau H} (\Pi e^{-i\tau H})^{m-1} | \psi_0 \rangle$ with $\Pi = \mathbf{1} - |\psi_0\rangle\langle\psi_0|$ as (cf. App. B)

$$\vec{\phi}_t = (\mathbf{1} + \Gamma)^{-1} \vec{v} \quad (17)$$

with the n -component vectors $\vec{\phi}_t = (\phi_{t,1}, \phi_{t,2}, \dots, \phi_{t,m})$, $\vec{v} = (v_1, v_2, \dots, v_m)$ and with the triangular matrix Γ whose elements are

$$\Gamma_{ij} = \begin{cases} u_{i-j} & 1 \leq i - j \leq m - 1 \\ 0 & \text{otherwise} \end{cases}. \quad (18)$$

In other words, the FDR/FDT amplitudes can be recursively constructed from the unitary amplitudes in Eq. (17). This is solved by a discrete Fourier transformation with

$$\sum_{m \geq 1} z^m \phi_{t,m} = \hat{\phi}_t(z) = \frac{\hat{v}(z)}{1 + \hat{u}(z)} \quad (19)$$

for z inside the complex unit disk (i.e., $|z| < 1$), and with the Fourier transformed unitary amplitudes of Eq. (16):

$$\hat{u}(z) = z \sum_{j=0}^N \frac{|\langle \Psi_0 | E_j \rangle|^2}{e^{iE_j\tau} - z}, \quad \hat{v}(z) = z \sum_{j=0}^N \frac{\langle \Psi | E_j \rangle \langle E_j | \Psi_0 \rangle}{e^{iE_j\tau} - z}. \quad (20)$$

The advantage of using a continuous function $\hat{\phi}_t(z)$ rather than a discrete function $\phi_{t,m}$ is that analytic tools, such as integration or perturbation theory, can be employed to exploit its properties.

Once the function $\hat{\phi}_t(z)$ is known, $\phi_{t,m}$ can be retrieved as the residue of the Cauchy integral: Since $\hat{\phi}(z)$ does not have poles inside the unit disk due to $1 + \hat{u} = \sum_j |\langle \Psi_0 | E_j \rangle|^2 / [1 - z \exp(-iE_j\tau)]$, the FDR/FDT amplitude reads

$$\phi_{t,m} = \frac{1}{2\pi i} \int_C z^{-m-1} \frac{\hat{v}}{1 + \hat{u}} dz \quad (21)$$

with a contour C around $z = 0$ smaller than the unit circle in order to avoid the poles of $\hat{v}/(1 + \hat{u})$. The function $\hat{\phi}_r = \hat{u}/(1 + \hat{u})$ is a uni-modular function of the form $\hat{\phi}_r(e^{i\omega}) = e^{if(\omega)}$ with a characteristic winding number that is equal to the dimensionality of the underlying Hilbert space in the absence of degeneracies for $E_j\tau \pmod{2\pi}$ [6]. The example of $N = 8$ non-interacting bosons is visualized in Fig. 1.

III. PHYSICAL MODEL: NON-INTERACTING BOSONS IN A DOUBLE WELL

Within the single mode approximation [42], the double well with N bosons can be described as a two-site Bose-Hubbard model,

$$H = -J(a_l^\dagger a_r + a_r^\dagger a_l) + \frac{U}{2}(n_l^2 + n_r^2), \quad (22)$$

where $a_{L,R}^\dagger$ ($a_{L,R}$) are the bosonic creation (annihilation) operators in the left/right potential wells, and $n_{l,r} = a_{l,r}^\dagger a_{l,r}$ are the corresponding number operators. J describes the tunneling of bosons between the two wells, and U represents the particle-particle interaction, which favors energetically a symmetric distribution of bosons in the double well when $U > 0$. Using Fock states $|n, N-n\rangle \equiv |n\rangle|N-n\rangle$ ($n = 0, \dots, N$) as a basis of the Hilbert space, the corresponding Hamiltonian matrix has a tridiagonal structure with

$$\begin{aligned} H_{n,n'} &= \langle n, N-n | H | n', N-n' \rangle \\ &= U[(N-n)^2 + n^2] \delta_{n,n'} - J\sqrt{n(N+1-n)} \delta_{n,n'-1} - J\sqrt{n'(N+1-n')} \delta_{n,n'+1}. \end{aligned} \quad (23)$$

These matrix elements represent an $(N+1)$ -site tight-binding chain with broken translational invariance, where the tunneling rate $-J\sqrt{n(N+1-n)}$ and the potential $U[(N-n)^2 + n^2]$ are minimal at the center and grow symmetrically towards the endpoints. The ‘sites’ n and n' are connected by hopping of a single particle. For the subsequent discussion we ignore the diagonal terms by setting $U = 0$, which gives us N non-interacting bosons in a double well.

For non-interacting bosons we can calculate $\hat{\rho}_{m;nn}$ explicitly, since the energy levels and the spectral weight factors $\langle n, N-n | E_k \rangle$ are known. This system can be realized for photons at a beam splitter [43, 44] or in two harmonic cavities, which are connected through an optical fiber [32–36]. Then the tunneling Hamiltonian $H = -J(a_l^\dagger a_r + a_r^\dagger a_l)$ for N bosons has $N+1$ equidistant energy levels $E_k = -J(N-2k)$ ($k = 0, 1, \dots, N$) with eigenstates

$$|E_k\rangle = \frac{2^{-N/2}}{\sqrt{k!(N-k)!}} (a_l^\dagger + a_r^\dagger)^k (a_l^\dagger - a_r^\dagger)^{N-k} |0, 0\rangle, \quad (24)$$

where the normalization follows directly from $(a^\dagger)^l |0\rangle = \sqrt{l!} |l\rangle$. Thus, the fastest oscillations occur with frequency NJ and the characteristic parameter for the evolution is $J\tau$.

The knowledge of the eigenstates enables us to calculate the spectral weights as scalar products

$$\begin{aligned} q_{n,k} &:= \langle n, N-n | E_k \rangle = \frac{2^{-N/2}}{\sqrt{k!(N-k)!}} \langle n, N-n | (a_l^\dagger + a_r^\dagger)^k (a_l^\dagger - a_r^\dagger)^{N-k} |0, 0\rangle \\ &= \frac{2^{-N/2}}{\sqrt{k!(N-k)!}} \langle n, N-n | \sum_{l=0}^k \binom{k}{l} (a_l^\dagger)^l (a_r^\dagger)^{k-l} \sum_{l'=0}^{N-k} \binom{N-k}{l'} (a_l^\dagger)^{l'} (-a_r^\dagger)^{N-k-l'} |0, 0\rangle, \end{aligned}$$

and since the left and right operators commute, we obtain after reordering

$$= \frac{2^{-N/2}}{\sqrt{k!(N-k)!}} \sum_{l=0}^k \binom{k}{l} \sum_{l'=0}^{N-k} \binom{N-k}{l'} (-1)^{N-k-l'} \langle n, N-n | (a_l^\dagger)^{l+l'} (a_r^\dagger)^{N-l-l'} |0, 0\rangle. \quad (25)$$

Due to the orthogonality of the states the sum vanishes unless $l+l' = n$. Then from the l summation there are two constraints for l' :

$$0 \leq l' = n-l, \quad n-l = l' \leq N-k,$$

which are equivalent to $n+k-N \leq l \leq n$, such that

$$\begin{cases} n+k-N \leq l \leq n & \text{for } n+k-N > 0 \\ 0 \leq l \leq n & \text{for } n+k-N \leq 0 \end{cases}.$$

This result, together with $(a^\dagger)^l |0\rangle = \sqrt{l!} |l\rangle$, implies for the scalar product

$$q_{n,k} = 2^{-N/2} \sqrt{\binom{N}{k} / \binom{N}{n}} \begin{cases} \sum_{l=0}^{\min\{k,n\}} \binom{k}{l} \binom{N-k}{n-l} (-1)^{N-k-n+l} & \text{for } n+k \leq N \\ \sum_{l=n+k-N}^{\min\{k,n\}} \binom{k}{l} \binom{N-k}{n-l} (-1)^{N-k-n+l} & \text{for } n+k > N \end{cases}. \quad (26)$$

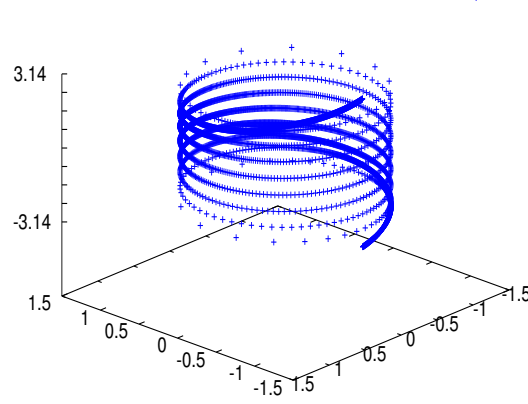


FIG. 1. $\hat{\phi}_r(e^{i\omega}) = e^{if(\omega)}$ for $-\pi \leq \omega < \pi$ (vertical axis) with winding number 9 for 8 non-interacting bosons. The density of points is inverse to the sensitivity of the phase $f(\omega)$ to a change of ω .

The orthonormal condition of the states $|n, N-n\rangle$ and the states $|E_k\rangle$, respectively, lead to

$$\sum_{n=0}^N q_{n,k} q_{n,k'} = \delta_{kk'} \quad \text{and} \quad \sum_{k=0}^N q_{n,k} q_{n',k} = \delta_{nn'}. \quad (27)$$

In particular, for the special cases $n=0$ and $n=N$ we have

$$q_{0,k} = 2^{-N/2} \frac{\sqrt{N!}}{\sqrt{k!(N-k)!}} (-1)^{N-k}, \quad q_{N,k} = 2^{-N/2} \frac{\sqrt{N!}}{\sqrt{k!(N-k)!}}. \quad (28)$$

These specific expressions can be entered into the FDR/FDT amplitude $\phi_{m;n0}$ of Eq. (12), using $D_k = e^{-iE_k\tau} = e^{iJ(N-2k)\tau}$. Moreover, Q_n , the diagonal matrix with elements $q_{n,k}$ for fixed n , is real here, which enables us to write

$$\phi_{m;n0} = \text{Tr}[D(D - Q_n E D Q_n)^{m-1} Q_0^* E Q_n] = \text{Tr}[D^{1/2} T^{m-1} D^{1/2} Q_0^* E Q_n]. \quad (29)$$

This gives immediately the reduced density matrix of Eq. (4), the EE of Eq. (6) and the ES of Eq. (7). Some examples for the eigenvalues of the monitored evolution matrix T are presented in Figs. 2, 3.

Returning to the unitary evolution, the amplitudes u_m and v_m of Eq. (16) are determined by a multiple of the frequency $J\tau$:

$$u_m = \langle 0, N | e^{-iHm\tau} | 0, N \rangle = \cos^N(mJ\tau), \quad v_m = \langle N, 0 | e^{-iHm\tau} | 0, N \rangle = (-i)^N \sin^N(mJ\tau), \quad (30)$$

which are periodic with $m\tau J/\hbar = 2\pi$ or periodic with $m\tau J/\hbar = \pi$ for even N (cf. Fig. 4). For a very short time (i.e., for $mJ\tau \ll 1/\sqrt{N}$) we have a Gaussian decay of the Fock state $|0, N\rangle$ as

$$u_m = \cos^N(mJ\tau) \sim e^{-Nm^2 J^2 \tau^2 / 2}, \quad (31)$$

as also illustrated in Fig. 4. This non-exponential behavior in τ reflects the quantum Zeno effect [45]. Finally, the Fourier transformed unitary amplitudes for $|\psi_0\rangle = |0, N\rangle$ and $|\psi\rangle = |N, 0\rangle$ read

$$\hat{u}(z) = 2^{-N} \sum_{k=0}^N \binom{N}{k} \frac{z}{e^{iE_k\tau} - z}, \quad \hat{v}(z) = (-2)^{-N} \sum_{k=0}^N \binom{N}{k} \frac{(-1)^k z}{e^{iE_k\tau} - z}. \quad (32)$$

They can be used to calculate the FDR/FDT amplitudes as the residue of the corresponding Cauchy integrals.

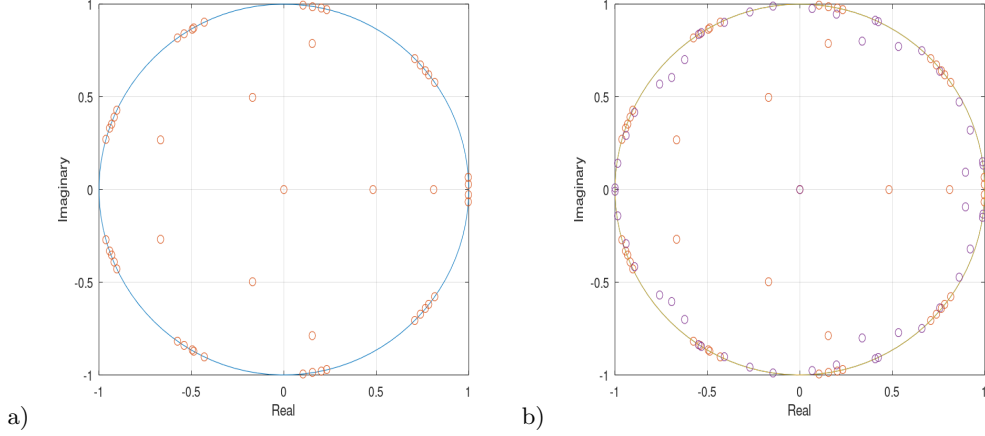


FIG. 2. 51 eigenvalues of T for $N = 50$ bosons. a) for $J\tau = 0.7\hbar$ and b) for $J\tau = 0.5\hbar$.

IV. DISCUSSION OF THE RESULTS

The results of the previous section will now be used to calculate the FDR/FDT probabilities, the EE and the ES for specific realizations of the model. To this end we note that the parameters of the bosonic system are the number of bosons N , the number of measurements $m - 1$ and the time steps between measurements τ . The latter always appears in the combination with the tunneling rate J as $J\tau$. This is a consequence of the fact that we have non-interacting bosons, where tunneling is the only mechanism of the evolution. The combination $J\tau/\hbar$ provides a dimensionless time step in our system, which we will use subsequently.

The characteristic features of the unitary dynamics defined in Eq. (30) is visualized in Fig. 4, which indicates a smooth variation of the amplitudes over time for the return to the initial state $|0, N\rangle \rightarrow |0, N\rangle$ and for the transition of all bosons to the other well $|0, N\rangle \rightarrow |N, 0\rangle$. This periodic behavior is also reflected by the unitary evolution of the EE in Fig. 5a, which vanishes when all bosons are either in the left or in the right well. Repeated measurements will substantially affect this periodic behavior.

entanglement entropy: Without measurement (i.e., for $m = 1$) the EE is determined by the unitary amplitudes for all transitions $|0, N\rangle \rightarrow |n, N - n\rangle$, which are smooth and periodic in time

$$\phi_{1,n0} = e^{iNJ\tau} \sum_{k=0}^N e^{-2ikJ\tau} q_{n,k} q_{0,k}. \quad (33)$$

This expression, together with Eq. (27), gives for $J\tau = 0 \pmod{2\pi}$ and $J\tau = \pi \pmod{2\pi}$

$$\phi_{1,n0} = e^{iNJ\tau} \delta_{n0}, \quad (34)$$

implying $\mathcal{S}_2(\tau, N, 1) = 0$. This is reflected in the plot of $\mathcal{S}_2(\tau, N, 1)$ of Fig. 5a, which indicates also a vanishing EE at $J\tau = \pi/2 \pmod{2\pi}$. The periodicity does not depend on the number of bosons N , while the value of the EE increases with N . This is remarkable because the eigenvalues as well as the weight $q_{n,k}$ depend strongly on N . The behavior of the EE is affected by measurements, depending on the time steps between the measurements. As visualized in Fig. 5b for $N = 20$ bosons, for a very short time step $J\tau$ between measurements the periodic behavior of the unitary evolution disappears. The corresponding entanglement spectra in Fig. 6 reveal that the level crossings are more complex in case of the monitored evolution and they take place on a much shorter time scale.

As already mentioned in the discussion of the FDR/FDT probabilities, the unitary evolution between measurements is characterized by the phase factors $\exp(-iJ\tau m/\hbar)$, which is periodic for $m = l$ if $J\tau/\hbar = 2\pi/l$. In other words, if the time step is a fraction of π , we expect a special behavior of the monitored evolution, which might be reminiscent of the periodic behavior of the unitary evolution. But how does the monitored evolution depend on l ? This we will analyze for $N = 4$ bosons, by comparing $l = 3$ and $l = 4$. Fig. 7 the four plots visualize how the ES changes from $J\tau/\hbar = \pi/l$ at the center to $\pi/l \pm 5 \cdot 10^{-5}$ at the boundaries. The left panels represent the ES for $m = 50$ measurements, the right panels the ES for $m = 51$ measurements. There are level degeneracies only at π/l , while in the narrow vicinity the levels are well separated and the spectrum is symmetric with respect to π/l . It should be noticed though that for $l = 4$ (Fig. 7a) the lowest level is two-fold degenerated, whereas for $l = 3$ (Fig. 7b) there is not such a degeneracy.

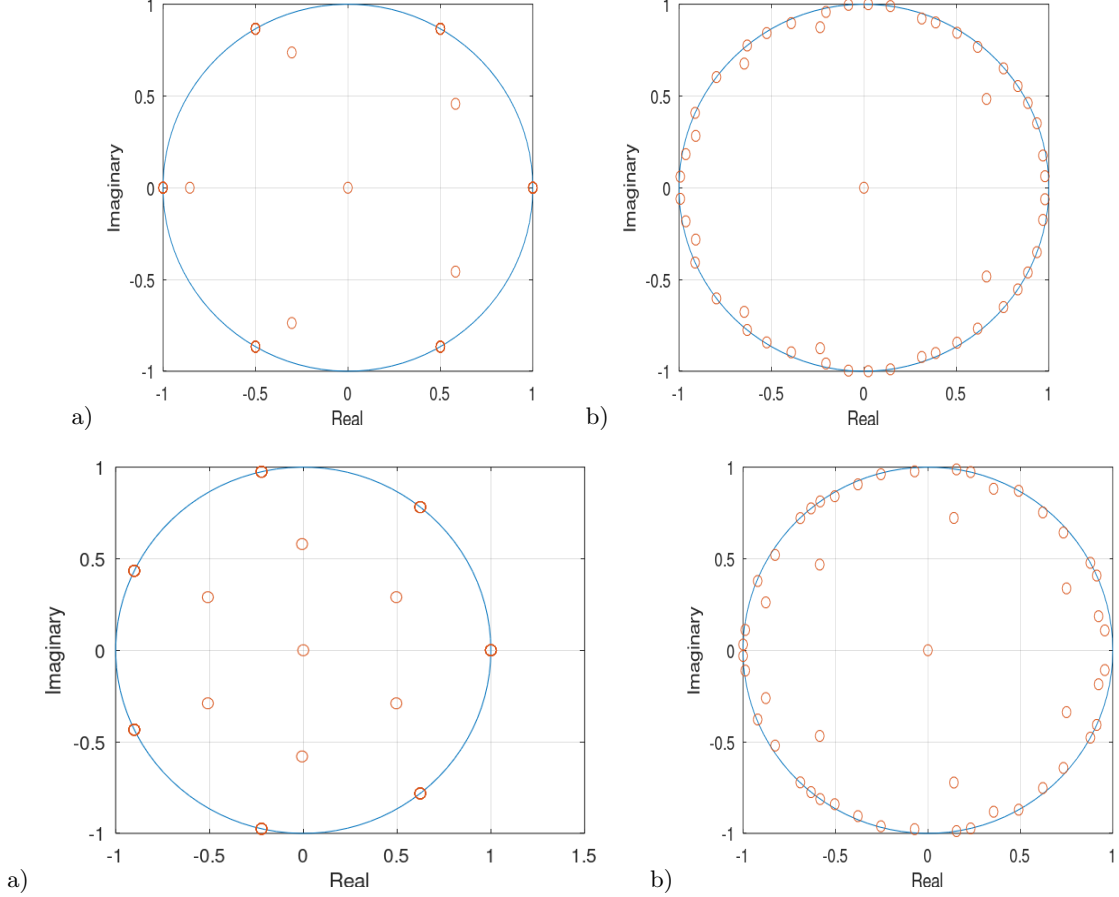


FIG. 3. 51 eigenvalues of T for $N = 50$ bosons. a) for $J\tau = (\pi/6)\hbar$, b) for $J\tau = (\pi/6 + 10^{-2})\hbar$ c) for $J\tau = (\pi/7)\hbar$ and d) for $J\tau = (\pi/7 + 10^{-2})\hbar$.

Another remarkable difference between $l = 3$ and $l = 4$ consists of the level change when the number of measurements changes from $m = 50$ (left) to $m = 51$ (right). While the lowest two levels for $l = 4$ are not affected by this change, there is a drastic change for $l = 3$. The latter has two low levels for $m = 50$ but three low levels for $m = 51$. The qualitative difference between these two m values reflects the fact that for an odd l only an odd m can satisfy the condition $mJ\tau/\hbar = 2\pi$ for periodicity of the phase factor. To understand the effect of this m -dependence on the EE, we use the definitions of the ES and the EE in Eqs. (6) and (7) and express the EE by the levels of the ES as

$$\mathcal{S}_2 = -\log_2 \left(\sum_{n=0}^N e^{-2\xi_{m;n}} \right), \quad (35)$$

where the sum is reminiscent to the sum of Boltzmann weights in statistical mechanics. Therefore, only small values of $\xi_{m;n}$ (i.e., low levels of the ES) contribute substantially to the EE. This means that the EE changes for $m \rightarrow m + 1$ when $l = 3$ but it remains unchanged for $l = 4$. This is what we see in Fig. 8. After some fluctuations for small values of m , the EE becomes stationary: For $l = 4$ there is just one stationary value (Fig. 8a), while for $l = 3$ the EE switches between two stationary values (Fig. 8b). The corresponding ES for $l = 3$ reflects the switching as a jump of levels between even and odd values of m , as illustrated for $m = 50$ and $m = 51$ in Fig. 7b. On the other hand, for $l = 4$ there is no level jump (Fig. 7a).

The above analysis relies on the fractional form $J\tau/\hbar = \pi/l$. The behavior of the EE for other values of the time step between measurements can change drastically and may lead to a strongly fluctuating behavior of the EE. In general, repeated measurements have two major effects on the evolution: they destroy the periodicity (recurrence) and they lead to more level crossings in the ES, as illustrated in Fig. 6. The origin of these effects is that the non-interacting bosons are coupled repeatedly in time to the measurement apparatus, which provides a similar effect as a local boson-boson interaction, since the measurement is performed on the same quantum state at different times. The situation can be compared with the unitary evolution of bosons with an interaction $U \neq 0$ in the Hamiltonian (22).

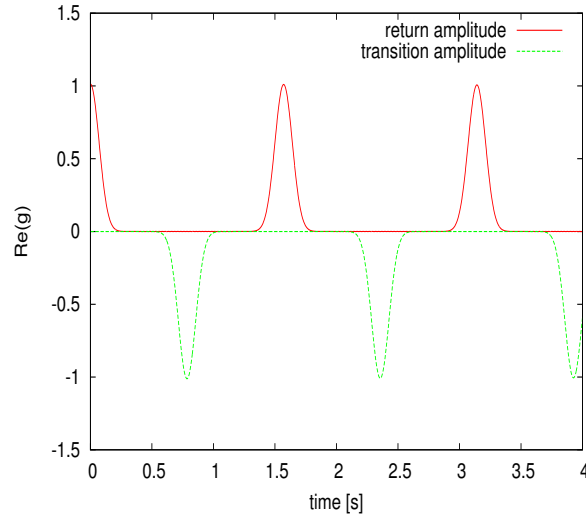


FIG. 4. Unitary evolution: Real parts of the return amplitude $u_1(\tau)$ ($|0, N\rangle \rightarrow |0, N\rangle$) and the transition amplitude $v_1(\tau)$ ($|0, N\rangle \rightarrow |N, 0\rangle$) as a function of the dimensionless time $J\tau/2\hbar$ for 50 non-interacting bosons.

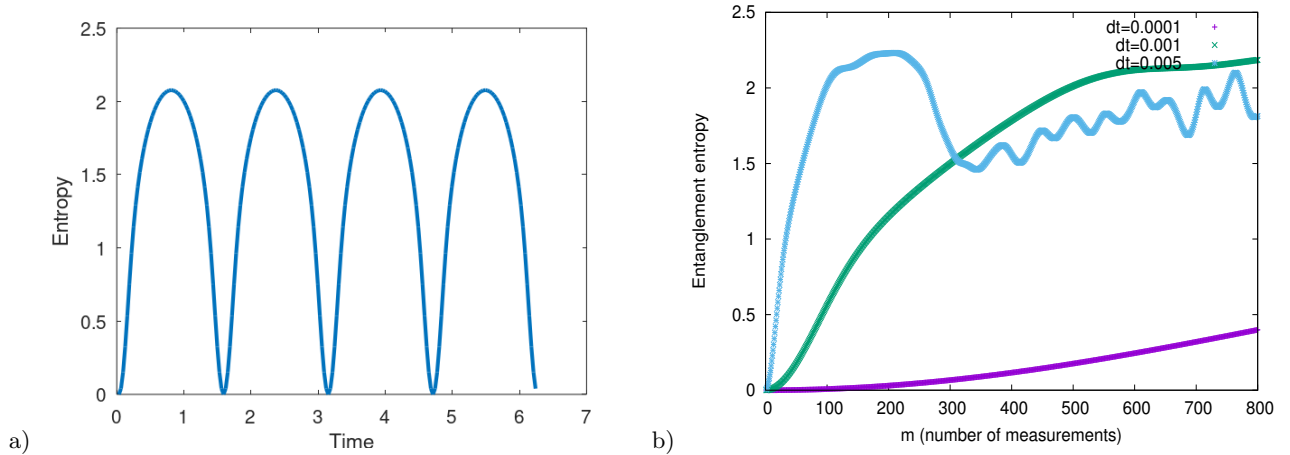


FIG. 5. a) The unitary evolution of $N = 20$ bosons for the time $J\tau/\hbar$ is periodic. b) The monitored evolution of the EE for a high frequency of measurements reflects the quantum Zeno effect, where an increasing measurement frequency reduces the EE.

We previously studied this system and found a similar behavior of a fluctuating EE and level crossings in the ES [27]. The fluctuations were removed by averaging over time intervals, an approach we could also apply in the present case with $U = 0$. For the monitored evolution we could also introduce random time steps between measurements and average over their distribution [41, 46–49]. As a disadvantage of such a time averaging, though, we would not be able to detect the switching of the EE in Fig. 8b).

V. CONCLUSION

We have studied the monitored evolution of N non-interacting bosons which tunnel between two wells. The monitoring is carried out by repeated projective measurements. The effect of these measurements is studied in terms of FDR/FDT probabilities to determine quantitatively the monitoring. From the FDR/FDT probabilities we have derived the reduced density matrix for one well, the EE and the ES. This is based on the relation (4) and enabled us to evaluate the EE and the ES directly from the FDR/FDT probabilities. It turns out that the EE is quite sensitive to a change of model parameters; i.e., on the number of bosons and the time step between two measurements. The rather complex behavior of the EE indicates that a single quantity, such as the EE, is quite limited for the characterization

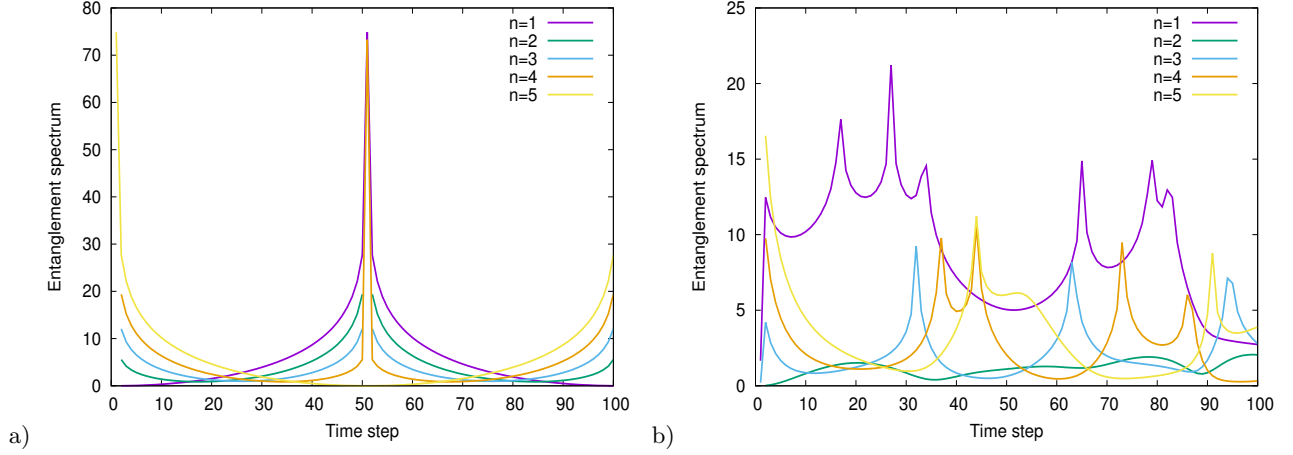


FIG. 6. The entanglement spectrum for the 5 levels of $N = 4$ bosons for $m = 1$ (a) and $m = 50$ (b) measurements as a function of the time step units $\pi J\tau/\hbar$ and $10^{-3}J\tau/\hbar$, respectively.

of the entanglement in the present system. More details are revealed by the ES of Eq. (7). It enables us to identify the statistical weight of each transition $|0, N\rangle \rightarrow |n, N-n\rangle$ to the monitored evolution individually. A characteristic feature of the ES is level crossing. Although it already appears in the unitary evolution (cf. Fig. 6a), it becomes much more complex for the monitored evolution in Fig. 6b) Except for the crossing points, there is always a unique lowest level, representing the dominant transition $|0, N\rangle \rightarrow |n, N-n\rangle$. The excitation to higher levels is important as long they are close to the lowest levels. This effect is important when the level $\xi_{m;n}$ changes quickly with m . This can happen near the special values $J\tau/\hbar = \pi/l$ (l integer), as demonstrated in Figs. 7.

Although our approach was employed only to non-interacting bosons, it is directly applicable to interacting bosons as well. New regimes might appear due to the competition of particle tunneling, particle-particle interaction and the interaction with the measurement apparatus. This is an ambitious project for the future, in which, among other aspects, the role of Hilbert-space localization should be addressed.

Acknowledgements

We are grateful to Eli Barkai for the useful discussions. This research is supported by the Israel Science Foundation through Grant No. 1614/21 (Q.L.).

Appendix A: Eigenstates

With the rotated basis $\{a_{\pm}, a_{\pm}^{\dagger}\}$:

$$a_{\pm}^{\dagger} := \frac{1}{2}(a_l^{\dagger} \pm a_r^{\dagger}), \quad a_{\pm} = \frac{1}{2}(a_l \pm a_r)$$

we obtain for the tunneling operator $a_l^{\dagger}a_r + a_r^{\dagger}a_l$

$$a_l^{\dagger}a_r + a_r^{\dagger}a_l = \frac{1}{2}[(a_l^{\dagger} + a_r^{\dagger})(a_l + a_r) - (a_l^{\dagger} - a_r^{\dagger})(a_l - a_r)] = \frac{1}{2}(a_+^{\dagger}a_+ - a_-^{\dagger}a_-), \quad (\text{A1})$$

where $(a_l^{\dagger} \pm a_r^{\dagger})(a_l \pm a_r)$ are number operators. Then we can directly show that a_+ and a_- and their Hermitean conjugate commute when a_l and a_r commute. As a consequence, the eigenstate reads

$$|E_k\rangle = \frac{2^{-N/2}}{\sqrt{k!(N-k)!}} (a_+^{\dagger})^k (a_-^{\dagger})^{N-k} |0, 0\rangle$$

and the application of the tunneling operator yields

$$\frac{1}{2}(a_+^{\dagger}a_+ - a_-^{\dagger}a_-)|E_k\rangle = (N - 2k)|E_k\rangle.$$

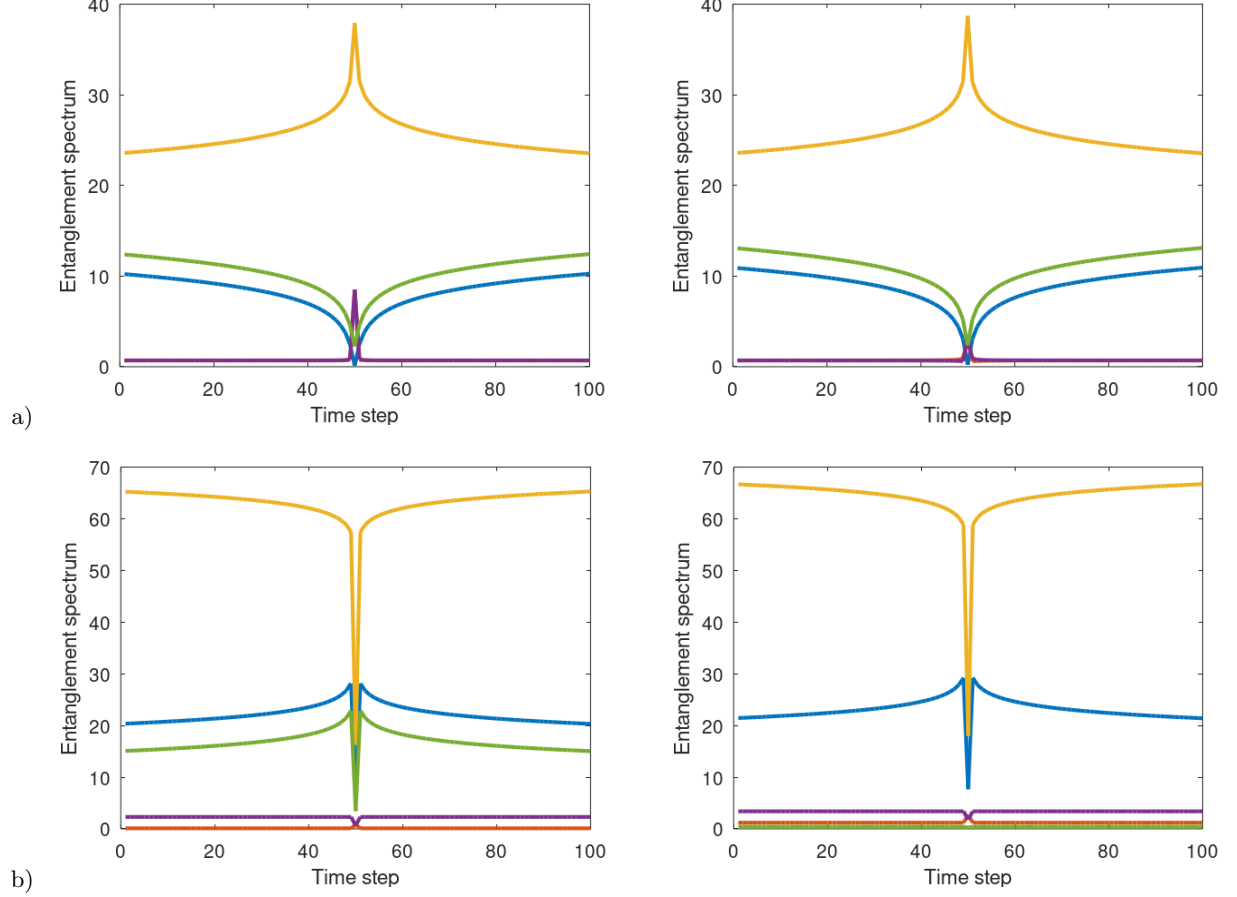


FIG. 7. Entanglement spectrum for $N = 4$ centered around $J\tau = \pi/4$ (a) and centered around $J\tau = \pi/3$ (b). The left panels present $m = 50$ measurements, the right panels $m = 51$ measurements. The jump of the green level in b) causes the switching effect of the entanglement entropy between two values, as illustrated in Fig. 8b. A unit of the time step on the abscissa is $10^{-7} J\tau/\hbar$.

Appendix B: Expansion of the first return/transition amplitude

Introducing the new notation for the FDR/FDT amplitude

$$\phi_{m+1,1} := \langle \psi | (e^{-i\tau H} \Pi)^m e^{-i\tau H} | \psi_0 \rangle = \langle \psi | e^{-i\tau H} (\Pi e^{-i\tau H})^m | \psi_0 \rangle, \quad \Pi = \mathbf{1} - |\psi_0\rangle\langle\psi_0|, \quad (\text{B1})$$

we obtain two equivalent recursion relations, namely

$$\phi_{m+1,1} = \phi'_{m,2} - u_1 \phi_{m,1} \quad \text{with} \quad \phi'_{m,k} = \langle \psi | e^{-ik\tau H} (\Pi e^{-i\tau H})^{m-1} | \psi_0 \rangle, \quad u_k = \langle \psi_0 | e^{-iHk\tau} | \psi_0 \rangle \quad (\text{B2})$$

from the third expression in Eq. (B1) and

$$\phi_{m+1,1} = \phi_{m,2} - \phi_{m,1} v_1 \quad \text{with} \quad \phi_{m,k} = \langle \psi | (e^{-i\tau H} \Pi)^{m-1} e^{-ik\tau H} | \psi_0 \rangle \quad (\text{B3})$$

from the second expression in Eq. (B1). Then the iteration of Eq. (B2) yields with $\phi_{t,m} \equiv \phi_{m,1}$

$$\phi_{t,m} = v_m - \sum_{j=1}^{m-1} u_{m-j} \phi_{t,j}, \quad \phi_{t,1} = v_1 \quad (\text{B4})$$

and the iteration of Eq. (B3)

$$\phi_{t,m} = v_m - \sum_{j=1}^{m-1} \phi_{t,m-j} v_j, \quad \phi_{t,1} = v_1. \quad (\text{B5})$$

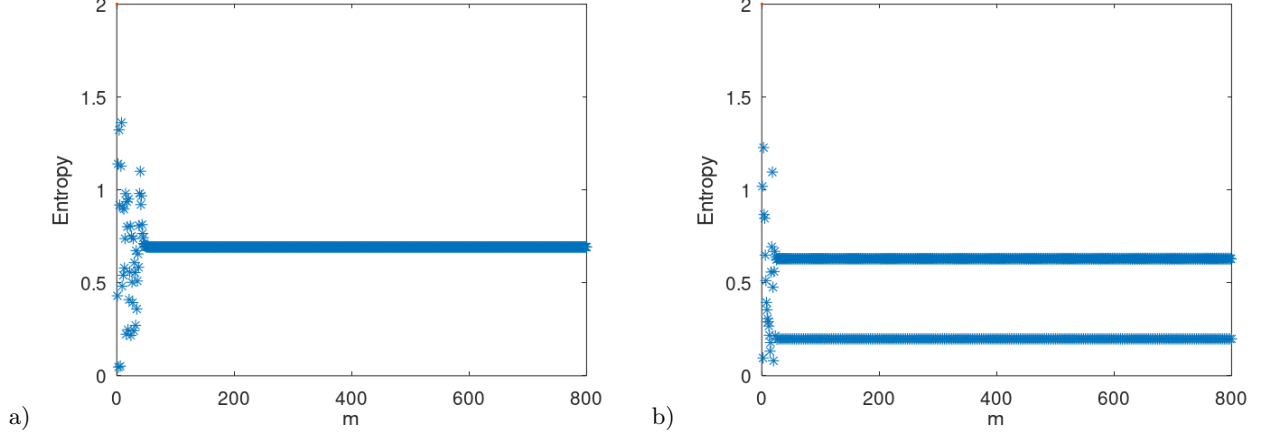


FIG. 8. The entanglement entropy for $N = 4$ is plotted for $J\tau = \pi/4$ (a) and $J\tau = \pi/3$ (b).

Using the vector notation $\vec{\phi}_t := (\phi_{t,1}, \phi_{t,2}, \dots, \phi_{t,m})$, $\vec{v} = (v_1, v_2, \dots, v_m)$, with the matrix Γ of Eq. (18) and with the matrix $\phi_t = (\phi_{t,m-j})$, we can write for Eqs. (B4) and (B5)

$$(\mathbf{1} + \Gamma)\vec{\phi}_t = \vec{v}, \quad \vec{\phi}_t = (\mathbf{1} - \phi_t)\vec{v}, \quad (\text{B6})$$

which yields $(\mathbf{1} - \phi_t)(\mathbf{1} + \Gamma) = \mathbf{1}$ and Eq. (17).

-
- [1] F. A. Grünbaum, L. Velázquez, A. H. Werner, and R. F. Werner. Recurrence for discrete time unitary evolutions. *Communications in Mathematical Physics*, 320(2):543–569, Jun 2013.
 - [2] Shrabanti Dhar, Subinay Dasgupta, and Abhishek Dhar. Quantum time of arrival distribution in a simple lattice model. *Journal of Physics A: Mathematical and Theoretical*, 48(11):115304, feb 2015.
 - [3] Shrabanti Dhar, Subinay Dasgupta, Abhishek Dhar, and Diptiman Sen. Detection of a quantum particle on a lattice under repeated projective measurements. *Phys. Rev. A*, 91:062115, Jun 2015.
 - [4] H Friedman, D A Kessler, and E Barkai. Quantum renewal equation for the first detection time of a quantum walk. *Journal of Physics A: Mathematical and Theoretical*, 50(4):04LT01, dec 2016.
 - [5] Sourabh Lahiri and Abhishek Dhar. Return to the origin problem for a particle on a one-dimensional lattice with quasi-zeno dynamics. *Phys. Rev. A*, 99:012101, Jan 2019.
 - [6] R. Yin, K. Ziegler, F. Thiel, and E. Barkai. Large fluctuations of the first detected quantum return time. *Phys. Rev. Research*, 1:033086, Nov 2019.
 - [7] Q. Liu, R. Yin, K. Ziegler, and E. Barkai. Quantum walks: The mean first detected transition time. *Phys. Rev. Research*, 2:033113, Jul 2020.
 - [8] Quancheng Liu, David A. Kessler, and Eli Barkai. Designing exceptional-point-based graphs yielding topologically guaranteed quantum search. *Phys. Rev. Res.*, 5:023141, May 2023.
 - [9] Luca Bombelli, Rabinder K. Koul, Joohan Lee, and Rafael D. Sorkin. Quantum source of entropy for black holes. *Phys. Rev. D*, 34:373–383, Jul 1986.
 - [10] Mark Srednicki. Entropy and area. *Phys. Rev. Lett.*, 71:666–669, Aug 1993.
 - [11] K. Audenaert, J. Eisert, M. B. Plenio, and R. F. Werner. Entanglement properties of the harmonic chain. *Phys. Rev. A*, 66:042327, Oct 2002.
 - [12] J. Eisert, M. Cramer, and M. B. Plenio. Colloquium: Area laws for the entanglement entropy. *Rev. Mod. Phys.*, 82:277–306, Feb 2010.
 - [13] Qiang Miao and Thomas Barthel. Eigenstate entanglement: Crossover from the ground state to volume laws. *Phys. Rev. Lett.*, 127:040603, Jul 2021.
 - [14] Luigi Amico, Rosario Fazio, Andreas Osterloh, and Vlatko Vedral. Entanglement in many-body systems. *Rev. Mod. Phys.*, 80:517–576, May 2008.
 - [15] Dmitry A. Abanin, Ehud Altman, Immanuel Bloch, and Maksym Serbyn. Colloquium: Many-body localization, thermalization, and entanglement. *Rev. Mod. Phys.*, 91:021001, May 2019.
 - [16] G. Vidal, J. I. Latorre, E. Rico, and A. Kitaev. Entanglement in quantum critical phenomena. *Phys. Rev. Lett.*, 90:227902, Jun 2003.
 - [17] Pasquale Calabrese and John Cardy. Entanglement entropy and quantum field theory. *Journal of Statistical Mechanics: Theory and Experiment*, 2004(06):P06002, jun 2004.

- [18] Ingo Peschel and Viktor Eisler. Reduced density matrices and entanglement entropy in free lattice models. *Journal of Physics A: Mathematical and Theoretical*, 42(50):504003, dec 2009.
- [19] Pasquale Calabrese and John Cardy. Entanglement entropy and conformal field theory. *Journal of Physics A: Mathematical and Theoretical*, 42(50):504005, dec 2009.
- [20] Maksym Serbyn, Z. Papić, and Dmitry A. Abanin. Criterion for many-body localization-delocalization phase transition. *Phys. Rev. X*, 5:041047, Dec 2015.
- [21] Rahul Nandkishore and David A. Huse. Many-body localization and thermalization in quantum statistical mechanics. *Annual Review of Condensed Matter Physics*, 6(1):15–38, 2015.
- [22] Pavel Kos, Marko Ljubotina, and Tomaž Prosen. Many-body quantum chaos: Analytic connection to random matrix theory. *Phys. Rev. X*, 8:021062, Jun 2018.
- [23] Amos Chan, Andrea De Luca, and J. T. Chalker. Solution of a minimal model for many-body quantum chaos. *Phys. Rev. X*, 8:041019, Nov 2018.
- [24] Yaodong Li, Xiao Chen, and Matthew P. A. Fisher. Measurement-driven entanglement transition in hybrid quantum circuits. *Phys. Rev. B*, 100:134306, Oct 2019.
- [25] Brian Skinner, Jonathan Ruhman, and Adam Nahum. Measurement-induced phase transitions in the dynamics of entanglement. *Phys. Rev. X*, 9:031009, Jul 2019.
- [26] Oliver Lunt, Marcin Sznyszewski, and Arijeet Pal. Measurement-induced criticality and entanglement clusters: A study of one-dimensional and two-dimensional clifford circuits. *Phys. Rev. B*, 104:155111, Oct 2021.
- [27] Quancheng Liu and Klaus Ziegler. Entanglement transition through hilbert-space localization. *Phys. Rev. A*, 107:012413, Jan 2023.
- [28] Aurel Bulgac. Entanglement entropy, single-particle occupation probabilities, and short-range correlations. *Phys. Rev. C*, 107:L061602, Jun 2023.
- [29] Aurel Bulgac, Matthew Kafker, and Ibrahim Abdurrahman. Measures of complexity and entanglement in many-fermion systems. *Phys. Rev. C*, 107:044318, Apr 2023.
- [30] Sabine Tornow and Klaus Ziegler. Measurement-induced quantum walks on an ibm quantum computer. *Phys. Rev. Res.*, 5:033089, Aug 2023.
- [31] Y. Minoguchi, P. Rabl, and M. Buchhold. Continuous gaussian measurements of the free boson CFT: A model for exactly solvable and detectable measurement-induced dynamics. *SciPost Phys.*, 12:009, 2022.
- [32] Tony E. Lee and M. C. Cross. Quantum-classical transition of correlations of two coupled cavities. *Phys. Rev. A*, 88:013834, Jul 2013.
- [33] S. Haroche, M. Brune, and J. M. Raimond. From cavity to circuit quantum electrodynamics. *Nature Physics*, 16(3):243–246, Mar 2020.
- [34] W. Löffler, T. G. Euser, E. R. Eliel, M. Scharrer, P. St. J. Russell, and J. P. Woerdman. Fiber transport of spatially entangled photons. *Phys. Rev. Lett.*, 106:240505, Jun 2011.
- [35] Yoonshik Kang, Jaekwon Ko, Sang Min Lee, Sang-Kyung Choi, Byoung Yoon Kim, and Hee Su Park. Measurement of the entanglement between photonic spatial modes in optical fibers. *Phys. Rev. Lett.*, 109:020502, Jul 2012.
- [36] Huan Cao, She-Cheng Gao, Chao Zhang, Jian Wang, De-Yong He, Bi-Heng Liu, Zheng-Wei Zhou, Yu-Jie Chen, Zhao-Hui Li, Si-Yuan Yu, Jacqueline Romero, Yun-Feng Huang, Chuan-Feng Li, and Guang-Can Guo. Distribution of high-dimensional orbital angular momentum entanglement over a 1 km few-mode fiber. *Optica*, 7(3):232–237, Mar 2020.
- [37] Y. Aharonov, L. Davidovich, and N. Zagury. Quantum random walks. *Phys. Rev. A*, 48:1687–1690, Aug 1993.
- [38] J. Bourgain, F. A. Grünbaum, L. Velázquez, and J. Wilkening. Quantum recurrence of a subspace and operator-valued schur functions. *Communications in Mathematical Physics*, 329(3):1031–1067, 2014.
- [39] H. Friedman, D. A. Kessler, and E. Barkai. Quantum walks: The first detected passage time problem. *Phys. Rev. E*, 95:032141, Mar 2017.
- [40] Hui Li and F. D. M. Haldane. Entanglement spectrum as a generalization of entanglement entropy: Identification of topological order in non-abelian fractional quantum hall effect states. *Phys. Rev. Lett.*, 101:010504, Jul 2008.
- [41] K Ziegler, E Barkai, and D Kessler. Randomly repeated measurements on quantum systems: correlations and topological invariants of the quantum evolution. *Journal of Physics A: Mathematical and Theoretical*, 54(39):395302, sep 2021.
- [42] G. J. Milburn, J. Corney, E. M. Wright, and D. F. Walls. Quantum dynamics of an atomic bose-einstein condensate in a double-well potential. *Phys. Rev. A*, 55:4318–4324, Jun 1997.
- [43] B. Yurke and D. Stoler. Generating quantum mechanical superpositions of macroscopically distinguishable states via amplitude dispersion. *Phys. Rev. Lett.*, 57:13–16, Jul 1986.
- [44] Serge Haroche and Jean-Michel Raimond. *Exploring the Quantum: Atoms, Cavities, and Photons*. Oxford University Press, 08 2006.
- [45] Baidyanath Misra and EC George Sudarshan. The zeno’s paradox in quantum theory. *Journal of Mathematical Physics*, 18(4):756–763, 1977.
- [46] Debraj Das, Sushanta Dattagupta, and Shamik Gupta. Quantum unitary evolution interspersed with repeated non-unitary interactions at random times: the method of stochastic liouville equation, and two examples of interactions in the context of a tight-binding chain. *Journal of Statistical Mechanics: Theory and Experiment*, 2022(5):053101, may 2022.
- [47] Debraj Das and Shamik Gupta. Quantum random walk and tight-binding model subject to projective measurements at random times. *Journal of Statistical Mechanics: Theory and Experiment*, 2022(3):033212, mar 2022.
- [48] Anish Acharya and Shamik Gupta. Tight-binding model subject to conditional resets at random times, 2023.
- [49] Manas Kulkarni and Satya N Majumdar. First detection probability in quantum resetting via random projective measurements. *Journal of Physics A: Mathematical and Theoretical*, 56(38):385003, sep 2023.